

Oxidative removal of metronidazole from aqueous solution by thermally activated persulfate process: kinetics and mechanisms

Rui Zhou¹ · Tingting Li¹ · Yu Su¹ · Taigang Ma¹ · Lijian Zhang¹ · Hejun Ren¹

Received: 15 August 2017 / Accepted: 18 October 2017 / Published online: 10 November 2017
© Springer-Verlag GmbH Germany 2017

Abstract Metronidazole (MNZ) is widely used in clinical applications and animal feed as an antibiotic agent and additive, respectively. Widespread occurrence of MNZ in wastewater treatment and hospital effluents has been reported. In this study, the mechanism of MNZ degradation in aqueous solutions via thermally activated persulfate (TAP) process was established under different conditions. The kinetic model was derived for MNZ degradation and followed pseudo-first-order reaction kinetics and was consistent with the model fitted by experimental data ($R^2 > 98.8\%$). The rate constant increased with the initial dosage of persulfate, as well as the temperature, and the yielding apparent activation energy was $23.9 \text{ kcal mol}^{-1}$. The pH of the solutions did not have significant effect on MNZ degradation. The degradation efficiency of MNZ reached 96.6% within 180 min for an initial MNZ concentration of 100 mg L^{-1} under the optional condition of $[\text{PS}]_0 = 20 \text{ mM}$, $T = 60 \text{ }^\circ\text{C}$, and unadjusted pH. SO_4^- and HO^\cdot were confirmed using electron paramagnetic resonance (EPR) spectra during TAP process. Radical quenching study revealed that SO_4^- was mainly responsible for MNZ degradation at an unadjusted pH. MNZ mineralization evaluation showed that the removal efficiency of total organic carbon (TOC) reached more than 97.2%.

Keywords Metronidazole · Thermal activation · Persulfate · Degradation · Kinetics · Sulfate radicals

Introduction

Metronidazole (MNZ, the properties of which is shown in Table 1) is a nitroimidazole antibiotic derivative that is often used in clinical applications and extensively used to prevent and treat infections caused by a wide range of bacteroides, anaerobic bacteria, and protozoal diseases, including trichomoniasis, gingivitis, amoebiasis, and vaginosis (Fang et al. 2010; Xiao et al. 2008). Moreover, MNZ is used as an additive in fish and poultry feed to eliminate parasites (Fang et al. 2011). Thus, MNZ is accumulated in animals, fish farm water, and wastewater from meat processing industries (Kümmerer 2001).

The maximum residual concentration of MNZ at 127 and 9400 ng L^{-1} has been found in wastewater treatment plants and hospital effluents, respectively (Rosal et al. 2010). Given its potential carcinogenic, mutagenic, and toxic properties, MNZ has adverse effects on humans and the ecological environment (Gómez et al. 2006). Moreover, MNZ is considerably difficult to be removed by employing traditional wastewater treatment methodologies and easily accumulates in the aquatic environment because of its high solubility and low biodegradability in water (Kümmerer et al. 2000). Therefore, the removal of MNZ from wastewater is of significant technical and environmental significance.

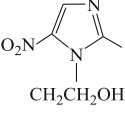
Several methods of MNZ removal from aqueous solutions have been reported, such as adsorption (Mendez-Diaz et al. 2010; Rivera-Utrilla et al. 2009), reduction of nanoscale zero-valent iron particles (Chen et al. 2012; Fang et al. 2011; Fang et al. 2010), Fenton processes (Shemer et al. 2006), ultrasound/photocatalysis/electrochemistry combined with

Responsible editor: Santiago V. Luis

✉ Hejun Ren
renhejun@jlu.edu.cn

¹ Key Laboratory of Groundwater Resources and Environment of the Ministry of Education, College of Environment and Resources, Jilin University, 2519 Jiefang Road, Changchun 130021, People's Republic of China

Table 1 Physical and chemical properties of MNZ

Molecular formula	C ₆ H ₉ N ₃ O ₃
Molecular weight (g mol ⁻¹)	171.15
Melting point (°C)	159–163
Water solubility (g L ⁻¹)	9.5
p <i>K</i> _a	2.55
Molecular structure	

Fenton process (Ammar 2016; Cheng et al. 2013; Shemer et al. 2006), ozonation technology (Sanchez-Polo et al. 2008), biological methods (Sanchez-Polo et al. 2008), and heterogeneous photocatalysis (Farzadkia et al. 2015). Investigating MNZ adsorption only examines its physical transformation process from water to solid phase and the MNZ that is eventually accumulated in the solid phase without any degradation, which is unsafe for the environment (Mendez-Diaz et al. 2010; Rivera-Utrilla et al. 2009). The reduction of nanoscale zero-valent iron particles and Fenton processes are greatly affected by the pH values of aqueous solution, and the methods perform well under low pH conditions (Chen et al. 2012; Shemer et al. 2006). The ozone/carbon system is efficient but with a low reactivity ozone (Sanchez-Polo et al. 2008). MNZ degradation via biological methods demands a long period of treatment, and the obtained degradation efficiency is generally extremely low (Ingerslev et al. 2001). Based on the above-described methods, exploring effective and feasible technologies to degrade MNZ in aqueous solutions is necessary.

Advanced oxidation process (AOP) has been proven effective in degrading organic pollutants in water. Traditional AOPs are based on the generation of highly oxidative hydroxyl radical (*HO*[•], *E*⁰ = 2.70 V) (Buxton et al. 1988). More recently, the reaction of sulfate radical (*SO*₄^{•-}, *E*⁰ = 2.5–3.1 V)-based AOPs with a series of pollutants, with a second-order-rate constant ranging from 10⁶ to 10⁹ M⁻¹ s⁻¹, has received increasing attention (Yan et al. 2013). In comparison with *HO*[•], *SO*₄^{•-} is considered to be more selective and less likely to be quenched by non-target water constituents because it can react with organic compounds mainly by electron transfer mechanism (Mahdi Ahmed et al. 2012). Persulfate (PS) is usually used to produce *SO*₄^{•-} because of its high aqueous solubility, high oxidative potential (*E*⁰ = +2.01 V), and high stability at room temperature (Ji et al. 2015). In addition, sulfate, which is the final product of PS, has minimal effect on microorganisms (Tsitonaki et al. 2008). *SO*₄^{•-} can be effectively generated by activating PS using initiators that include heat, ultrasound, microwaves, UV light, and transition metals (Meⁿ⁺) (Weng and Tsai 2016; Yan et al. 2011).

Among various activation methods, thermally activated persulfate (TAP) is worth investigating. In TAP process, PS is commonly used as a precursor that leads to *SO*₄^{•-} formation via homolysis of peroxide bond, which further oxidizes the organic compounds (Tsitonaki et al. 2010). Several previous studies have documented the effectiveness of TAP oxidation of antibiotics (Fan et al. 2015; Gao et al. 2016), herbicides (Ji et al. 2015; Tan et al. 2012), and industrial chemicals (Gu et al. 2011). The TAP process offers some advantages compared with other methods. For example, it can minimize the consumption of PS during pre-mixing with other activators because it has no added chemicals. In addition, the TAP process is commonly employed in evaluating the reaction mechanism between pollutants and free radicals due to its simplicity and high efficiency (Antoniou et al. 2010). However, the effect of the TAP process on MNZ degradation has not yet been investigated.

In the present study, control experiments were conducted to evaluate the practicability of employing the TAP process on MNZ degradation. The study aims to explore a feasible method in removing and even mineralizing MNZ in aqueous solutions. Kinetic studies were performed to explore the influence factors, including the initial PS concentration, temperature, and pH. The dominant reactive radicals were identified through ERP experiment, derivation of the kinetic modeling, and radical quenching study to reveal the degradation mechanism of MNZ.

Materials and methods

Chemicals

The following chemicals used were of analytical reagent grade and purchased from Sinopharm Chemical Reagent Co., China: MNZ (99%), PS (Na₂S₂O₈, ≥ 98.0%), 5,5-dimethyl-1-pyrrolidine *N*-oxide (DMPO, C₆H₁₁NO, 99.0%, for EPR spectroscopy), sulfuric acid (H₂SO₄, 95–98%), sodium hydroxide (NaOH, ≥ 96.0%), sodium bicarbonate (NaHCO₃, ≥ 99.5%), methanol (MeOH, CH₄O, ≥ 99.5%), and *tert*-butyl alcohol (TBA, C₄H₁₀O, ≥ 98.0%). All chemical reagents were intrinsically used without further purification, and all stock solutions were prepared with ultrapure water from a Millipore system.

Experimental produce

MNZ degradation was studied through batch experiments in a range of 100-mL closed bottles containing 60 mL of the reaction solution. The bottles were incubated in a stirring water bath reactor at a determinate temperature under 150 rpm for 180 min. Given that the concentration limit of MNZ is higher

than its aqueous environmental, a relatively high initial concentration of MNZ was selected at 100 mg L^{-1} to explore its degradation trend and kinetics in the batch oxidation experiment. Different factors that affect the degradation efficiency of MNZ were investigated, including the initial PS dosage, temperature, and initial pH values. The initial pH values in all solutions were unadjusted. However, pH values were adjusted by adding $0.1 \text{ M H}_2\text{SO}_4$ or NaOH to investigate the influence of the initial pH value. Control experiments without PS or heat were also conducted under identical conditions. Different concentrations of quenchers were added to the reaction solutions (including MeOH and TBA) at specific pH values to identify the dominant reactive radicals in the solutions. Aliquots (0.2 mL) of the samples were withdrawn from the reactor at selected time intervals and quenched immediately with an appropriate volume of MeOH (0.5 mL), a quenching reagent for $\text{SO}_4^{\cdot-}$ and HO^{\cdot} (Chen et al. 2016). At the same time, samples were chilled in an ice bath for at least 30 min to prevent further MNZ degradation (Fan et al. 2015; Olmez-Hanci et al. 2013). The pH values of the samples should be adjusted at the same level (approximately 0.3) by adding $0.1 \text{ M H}_2\text{SO}_4$ (3.3 mL) before analysis. All the experiments were conducted in triplicates or more, and the average values were used; the standard deviations were limited to $< 10\%$.

Analytical methods

MNZ concentration was quantified by a UV–visible spectrophotometer (T6 New Century, Beijing) at the wavelength of 277 nm (Azam et al. 2011; Szente et al. 2011). PS concentration was analyzed according to the spectrophotometric method proposed by Liang et al. (2008). Solution pH was measured using a pH meter (Sartorius PB-10, Germany). By using DMPO as a spin trap, $\text{SO}_4^{\cdot-}$ and HO^{\cdot} were identified with an EPR spectrometer (JES-FA spectrometer/X band). TOC was monitored using a TOC analyzer (Shimadzu SSM-5000A, Japan). Determining TOC content requires a large number of samples; thus, the same sample was withdrawn without quencher from the three bottles under the same conditions, mixed well, and then filtered through a $0.45\text{-}\mu\text{m}$ membrane before measurement.

Results and discussion

Effectiveness of the TAP process for MNZ degradation

A series of comparative experiments was performed to identify the effectiveness of the TAP process for MNZ degradation. These batch experiments were conducted in the same reactor and controlled under the same experimental conditions. Figure 1 shows the performance of MNZ degradation

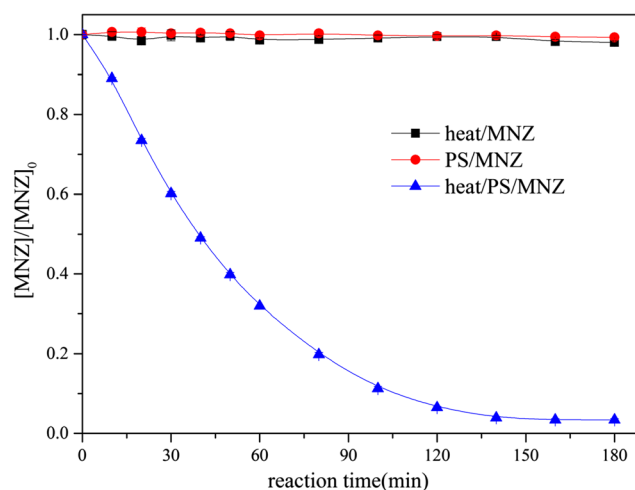
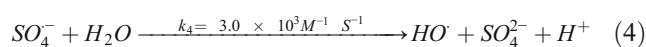
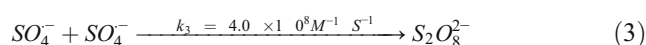
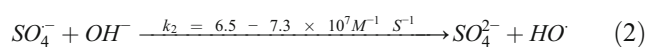


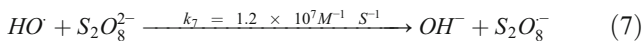
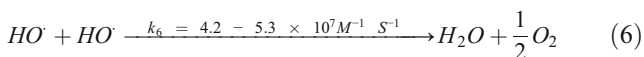
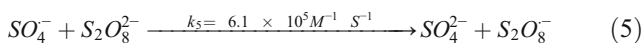
Fig. 1 Degradation of MNZ in different comparison blank experiments (unadjusted pH, $T = 60 \text{ }^\circ\text{C}$, $[\text{PS}]_0 = 20 \text{ mM}$, $[\text{MNZ}]_0 = 100 \text{ mg L}^{-1}$)

in PS solution or heat alone and in PS coupled with heat. The results indicate that MNZ can stably exist for 180 min or more without PS or at room temperature. By contrast, adding PS in the TAP process resulted in rapid and pronounced MNZ degradation, with 96.6% removal during the 180-min reaction time. Therefore, MNZ degradation occurred in the presence of PS and heat but not of PS or heat alone. The results prove that reactive free radicals can efficiently induce TAP process. The TAP process can produce $\text{SO}_4^{\cdot-}$ and HO^{\cdot} sequentially. Thus, these free radicals may result in a decreased MNZ concentration. Although PS is a strong oxidant with a high oxidative potential, it cannot react with MNZ at room temperature. However, $\text{SO}_4^{\cdot-}$ was induced by the TAP process with a high redox potential. Produce of these free radicals can greatly accelerate the kinetics of oxidation on MNZ degradation.

Kinetic modeling of MNZ degradation

A kinetic modeling study was conducted because of the planned experimental conditions. A typical oxidation of contaminants based on PS activation can be described as the following three key reactions: (1) $\text{SO}_4^{\cdot-}$ generation from PS activation, as indicated in Eq. (1); (2) transformation from $\text{SO}_4^{\cdot-}$ into HO^{\cdot} or the consumption of free radicals, except in MNZ degradation, as shown in Eqs. (2–7); and (3) degradation of target organic compound by dominant radicals, as expressed in Eqs. (8–9).





To evaluate the kinetic models of these degradation reactions, MNZ was assumed to be mainly degraded by SO_4^- and HO^\cdot . The corresponding kinetic equation for MNZ and the free radicals can be expressed as follows (Eqs. (10–12)):

$$\frac{d[MNZ]}{dt} = -k_8 [SO_4^-] [MNZ] - k_9 [HO^\cdot] [MNZ] \quad (10)$$

$$\frac{d[SO_4^-]}{dt} = k_1 [S_2O_8^{2-}] - k_2 [SO_4^-] [OH^-] - k_3 [SO_4^-]^2 - k_4 [SO_4^-] [H_2O] - k_5 [SO_4^-] [S_2O_8^{2-}] - k_8 [SO_4^-] [MNZ] \quad (11)$$

$$\frac{d[HO^\cdot]}{dt} = k_2 [SO_4^-] [OH^-] + k_4 [SO_4^-] [H_2O] - k_6 [HO^\cdot]^2 - k_7 [HO^\cdot] [S_2O_8^{2-}] - k_9 [HO^\cdot] [MNZ] \quad (12)$$

The rate constants of Reactions (4) and (5) are evidently lower than those of other reactions consuming SO_4^- ; thus, the rate constants of Reactions (4) and (5) can be neglected in the side reaction. Similarly, the rate constants of Reaction (4) are significantly lower than those of other reactions depleting HO^\cdot . $[SO_4^-]$ and $[HO^\cdot]$ are constants and do not change with time when these reactions reach equilibrium. The reaction can be simplified as follows (Eqs. (13–14)):

$$\frac{d[SO_4^-]}{dt} = k_1 [S_2O_8^{2-}] - k_8 [SO_4^-] [MNZ] - \sum_i k_i [S_i] [SO_4^-] = 0 \quad (13)$$

$$\frac{d[HO^\cdot]}{dt} = k_2 [SO_4^-] [OH^-] - k_9 [HO^\cdot] [MNZ] - \sum_j k_j [S_j] [HO^\cdot] = 0 \quad (14)$$

where $[S_i]$ represents the SO_4^- quenchers, including SO_4^- and OH^- , and $[S_j]$ represents the quenchers of HO^\cdot , including HO^\cdot and $S_2O_8^{2-}$.

PS concentration should be sufficient to degrade pollutants completely and avoid free radical scavengers. Under the optimal experimental conditions, MNZ concentration is lower than that the other scavengers. Thus, $[SO_4^-]$ and $[HO^\cdot]$ can be derived as follows (Eqs. (15–16)):

$$[SO_4^-] = \frac{k_1 [S_2O_8^{2-}]}{k_8 [MNZ] + \sum_i k_i [S_i]} = \frac{k_1 [S_2O_8^{2-}]}{\sum_i k_i [S_i]} \quad (15)$$

$$[HO^\cdot] = \frac{k_2 [SO_4^-] [OH^-]}{k_9 [MNZ] + \sum_j k_j [S_j]} = \frac{k_2 [SO_4^-] [OH^-]}{\sum_j k_j [S_j]} \quad (16)$$

Equation (1) can be converted as Eq. (17):

$$\begin{aligned} \frac{d[MNZ]}{dt} &= -k_8 \frac{k_1 [S_2O_8^{2-}]}{\sum_i k_i [S_i]} [MNZ] - k_9 \frac{k_2 [SO_4^-] [OH^-]}{\sum_j k_j [S_j]} [MNZ] \\ &= -k_8 \frac{k_1 [S_2O_8^{2-}]}{\sum_i k_i [S_i]} [MNZ] - k_9 \frac{k_2 [OH^-]}{\sum_j k_j [S_j]} \cdot \frac{k_1 [S_2O_8^{2-}]}{\sum_i k_i [S_i]} [MNZ] \\ &= - \left(k_8 + k_9 \frac{k_2 [OH^-]}{\sum_j k_j [S_j]} \right) \cdot \frac{k_1 [S_2O_8^{2-}]}{\sum_i k_i [S_i]} [MNZ] \end{aligned} \quad (17)$$

The simplified form of Eq. (17) is shown below.

$$\frac{d[MNZ]}{dt} = -k_{obs} [MNZ] \quad (18)$$

The integrated form of Eq. (18) is shown below.

$$\ln \left(\frac{[MNZ]}{[MNZ]_0} \right) = -k_{obs} t \quad (19)$$

Therefore, the relationship between $\ln([MNZ]/[MNZ]_0)$ and the reaction time t is linear and follows the pseudo-first-order reaction kinetic model. The kinetic model derived did not only analyze the degradation process but also verified the proposed model fitted by experimental data in this work.

Effect of initial PS dosage

The effect of different PS dosages (10, 20, 30, 40, and 50 mM) on the degradation rate of MNZ was investigated at an optimized temperature of 60 °C and unadjusted pH, and the experimental results are shown in Fig. 2a. From the figure, MNZ concentration decreased obviously over time. Within the same reaction time, the total degradation efficiency of MNZ increased significantly with the increase of PS concentration from 10 to 30 mM, and high degradation efficiencies were obtained with high PS concentration. However, for high concentration of PS, the percentage of MNZ degradation slightly decreased when the PS concentration reached 50 mM. Excessive SO_4^- can be generated at excess PS concentrations; thus, the recombination of sulfate radicals and their reaction with H_2O , $S_2O_8^{2-}$, as well as their reaction with each other and as scavengers (Eqs. (3–5)), diminish the efficiency of MNZ degradation (Lee et al. 2012; Wang et al. 2014). As shown in Fig. 2b, degradation of MNZ could be well-fitted to the pseudo-first-order kinetic model at different PS dosage. The degradation rate constant of MNZ k_{obs} (i.e., the value obtained by linear regression of $\ln([MNZ]/[MNZ]_0)$ versus t) plot

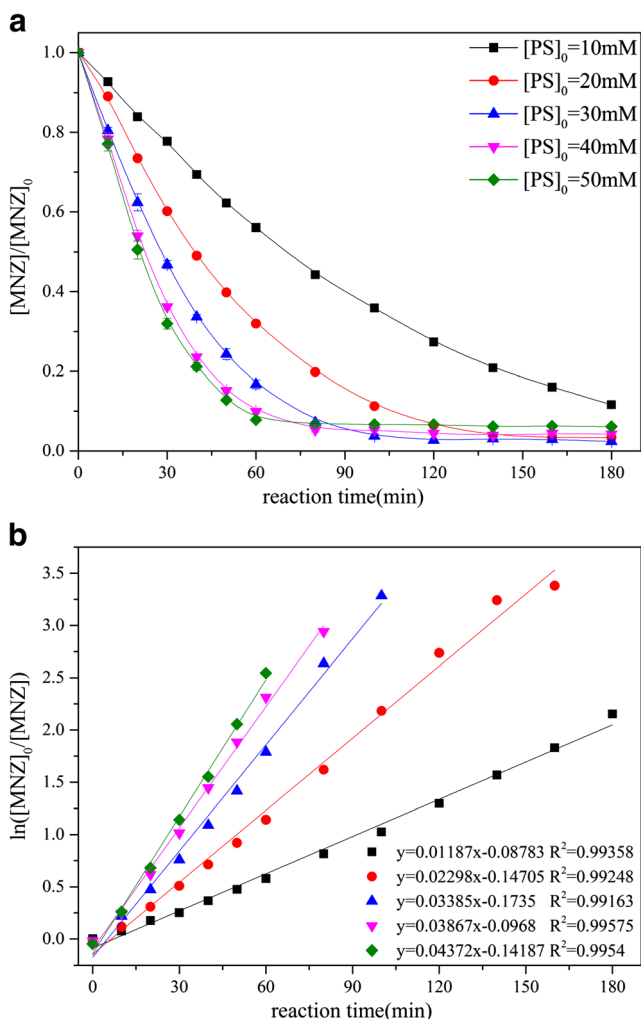


Fig. 2 a Effect of initial persulfate dosage on MNZ degradation. b The pseudo-first-order kinetic reaction equations derived from a (unadjusted pH, $T = 60\text{ }^{\circ}\text{C}$, $[\text{MNZ}]_0 = 100\text{ mg L}^{-1}$)

increased from 0.012 to 0.044 min^{-1} , and half-lives decreased from 58.39 to 15.85 min (calculated by Eq. (20)) when the PS concentration increased from 10 to 50 mM . This result is caused by the PS concentration directly affecting the equilibrium concentration of $[\text{SO}_4^-]$ (Ghauch et al. 2012; Ji et al. 2015).

$$t_{\frac{1}{2}} = \frac{\ln 2}{k_{obs}} \quad (20)$$

Based on the PS dosage being proportional to the degradation rate constant, the increase in PS concentration could enhance the degradation rate constant. The TAP process could yield SO_4^- , which participates in the oxidation reaction and MNZ degradation. Obviously, TAP process could generate more SO_4^- when more initial PS concentration is added into the reaction process, thereby enhancing degradation rate, which is in accordance with the results obtained in the

literature (Chen et al. 2016). The calculated rate constants k_{obs} were well-fitted with the pseudo-first-order kinetic model, as made evident by the high linear correlation coefficient ($R_2 > 0.99$). In view of economic efficiency, 20 mM PS was selected as the optimal PS concentration for 100 mg L^{-1} MNZ degradation.

Effect of temperature

Temperature plays an important role in the TAP process. It determines the decomposition of PS and the amount of SO_4^- (Deng et al. 2013). Therefore, the influence of temperature on MNZ degradation trend was evaluated by varying activation temperatures (i.e., 50 , 60 , 70 , and $80\text{ }^{\circ}\text{C}$) at an optimized PS dosage of 20 mM and unadjusted pH. As shown in Fig. 3a, MNZ degradation rate obviously enhanced with the increasing temperature. Thus, high temperature is beneficial to MNZ degradation. The results show that MNZ degradation weakened at $50\text{ }^{\circ}\text{C}$ and that the degradation efficiency of MNZ was only 56.1% at a reaction time of 180 min . However, the degradation efficiency of MNZ significantly increased with the increase in temperature from 60 to $80\text{ }^{\circ}\text{C}$. Over 90% MNZ degradation was obtained at 80 , 70 , and $60\text{ }^{\circ}\text{C}$ within 25 , 40 , and 120 min , respectively. Meanwhile, the degradation efficiency of MNZ was 6.7 , 26.6 , 71.8 , and 84% at 50 , 60 , 70 , and $80\text{ }^{\circ}\text{C}$, respectively, for the reaction time of 20 min . This phenomenon is typical for the TAP process, during which more free radicals can be generated through thermal energy for the degradation of target contaminants at higher temperature and considerably increasing the degradation rate (Ghauch et al. 2012). Therefore, the TAP process can reduce the reaction time by increasing the reaction temperature.

At each temperature, the calculated reaction rate constant by the MNZ degradation trend was observed to be well-fitted with the pseudo-first-order kinetics model ($R^2 > 99\%$), and the experimental results are shown in Fig. 3b. Moreover, the obtained degradation rate constant of MNZ increased from 0.0046 to 0.10 min^{-1} , and half-lives decreased from 149.71 to 6.74 min when the reaction temperature increased from 50 to $80\text{ }^{\circ}\text{C}$. The k_{obs} value evidently increased with the increase of reaction temperature based on thermodynamic principle. The temperature dependency of k_{obs} was further investigated using the Arrhenius equation, as shown as follows (Eq. (21)):

$$\ln k_{obs} = \ln A - \frac{E_a}{RT} \quad (21)$$

where A is the pre-exponential (or frequency) factor, E_a is the apparent global activation energy (J mol^{-1}), R is the universal gas constant ($1.99\text{ cal mol}^{-1}\text{ K}^{-1}$), and T is the absolute temperature (K).

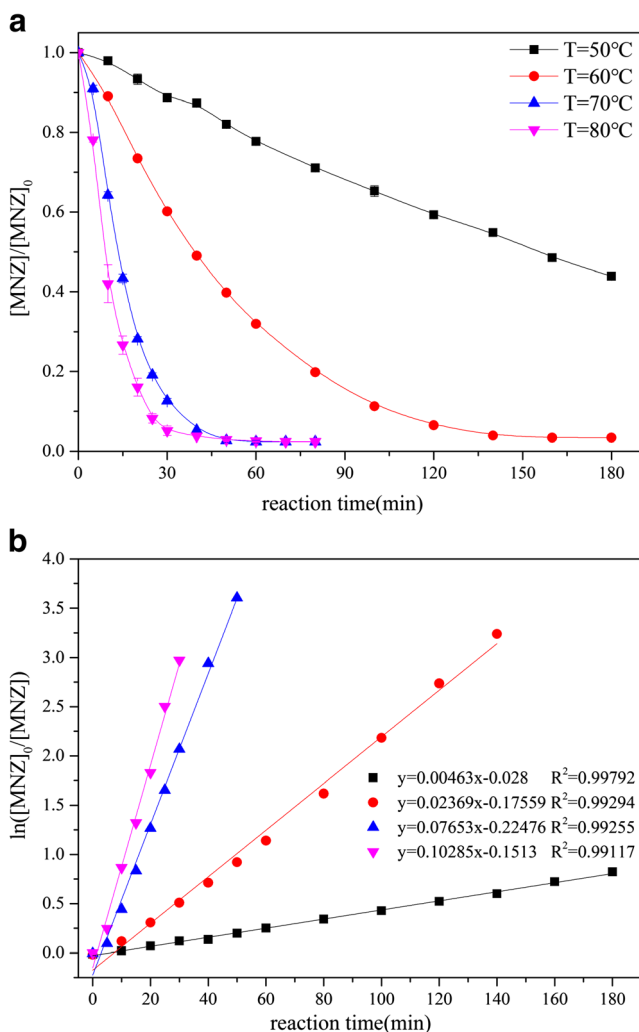


Fig. 3 **a** Effect of reaction temperature on MNZ degradation. **b** The pseudo-first-order kinetic reaction equations derived from **a** (unadjusted pH, [PS]₀ = 20 mM, [MNZ]₀ = 100 mg L⁻¹)

According the Arrhenius equation, the activation energy E_a was determined to be 23.9 kcal mol⁻¹ over the range of 50–80 °C. This value of E_a is lower than other previously reported contaminants (e.g., 25.8 ± 0.7 kcal mol⁻¹ for trichloroethene (Gómez et al. 2007), 39.8 ± 0.2 kcal mol⁻¹ for diuron (Tan et al. 2012), and 40.1 kcal mol⁻¹ for ibuprofen oxidation (Ghauch et al. 2012). This comparison indicates that the TAP process easily oxidizes MNZ molecules.

For a deeper understanding, activation enthalpy ΔH and activation entropy ΔS could be calculated simultaneously by Eqs. (22–23), wherein Eq. (22) is the Eyring–Polanyi equation. The general form of the equations is expressed as follows:

$$k_{obs} = \frac{k_B T}{h} \exp\left(-\frac{\Delta G}{RT}\right) \tag{22}$$

$$\Delta G = \Delta H - T \cdot \Delta S \tag{23}$$

By substituting Eq. (23) in Eq. (24), the Eyring–Polanyi equation can be expressed as:

$$\ln \frac{k_{obs}}{T} = -\frac{\Delta H}{R} \cdot \frac{1}{T} + \ln \frac{k_B}{h} + \frac{\Delta S}{R} \tag{24}$$

where k_{obs} is the rate constant, k_B is the Boltzmann constant (3.3×10^{-24} cal K⁻¹), T is the absolute temperature (K), h is the Planck constant (1.58×10^{-34} cal s), ΔG is the Gibbs energy of activation, and R is the universal gas constant (1.99 cal mol⁻¹ K⁻¹).

According to Eq. (14), the plot of $\ln(k_{obs}/T)$ versus $1/T$ fits out of a straight line, wherein $-\Delta H/R$ is the slope and $\ln(k_B/h) + \Delta S/R$ is the intercept, from which the values of ΔH and ΔS could be calculated as 23.2 kcal mol⁻¹ and 3.08 cal mol⁻¹ K⁻¹, respectively.

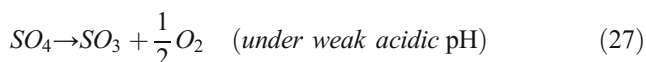
The result confirms that the TAP process can increase the reaction rate and reduce half-life by increasing the reaction temperature. Thus, temperature plays a critical role in the TAP process. Although higher radicals can be generated in a short period of time at a high temperature, which can promote MNZ degradation, elevated scavenging reactions and fast PS consumption may occur simultaneously (Peyton 1993). This phenomenon was not evident in this study, which might be due to the relatively low concentration of PS used in the experiment. Therefore, determining an optimal temperature is essential for the target contaminant degradation. In view of all these factors, 60 °C was selected as the optimal temperature for MNZ degradation.

Effect of initial pH

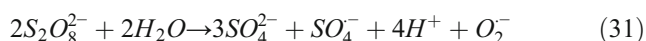
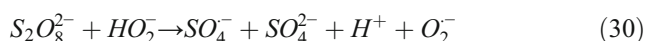
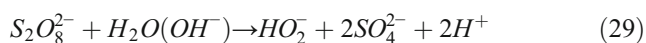
pH plays a complex role and influences the generation of various free radicals of target contaminants during TAP oxidation (Nie et al. 2014). At the same time, varying pH values can influence the speciation and functional groups of pollutants differently, thereby affecting the mechanisms of pollutant degradation. The mechanism of uncatalyzed, acid-catalyzed (Kolthoff and Miller 1951), and basic-activated reactions (Furman et al. 2010) is advanced for the thermal decomposition of PS on target contaminant degradation in aqueous solutions. The uncatalyzed reaction was conducted using the TAP process and the generated reaction radicals in this work (as described by Eqs. (1), (4), and (6)). Acid-catalyzed reaction could deplete PS concentration through non-radical pathways without SO_4^- generation under acidic conditions, and PS had different consumption pathways at a strong and weak acidic pH (as described by Eqs. (25–27). However, SO_4^- generation could be inhibited by ineffective anions formed at a strong acidic condition (Eq. (28)) (McCallum et al. 2000). Most studies have shown that basic-activated PS is also an effective method for pollutant degradation (Yifei and Shaojin 2008). Under basic conditions, the generated SO_4^-

can also be transformed into $HO\cdot$ by reacting with OH^-/H_2O (Eqs. (2) and (4)) with different chemical equilibrium constants (Liang et al. 2007). Apart from these reaction pathways, some studies have also mentioned that $S_2O_8^{2-}$ can produce HO_2^- by initially reacting with OH^- . HO_2^- generation has an intermediate interaction with PS, which forms the cleavage of O–O in PS molecule and generates SO_4^- under base activation in the solution (Eqs. (29–31)) (House 1962; Singh and Venkatarao 1976).

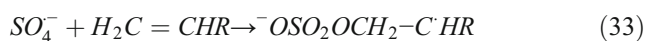
Acid-catalyzed reaction



Basic-activated reaction



The mechanism of contaminant degradation was affected by the composition of effective substances at different pH values. The reaction mechanism of different reactive radicals with functional groups of different organic compounds could be slightly different, which also influences the degradation of target contaminants. For example, different from the mechanism by $HO\cdot$, which attacks organic pollutants, $HO\cdot$ principally reacts by adding to C=C double bonds, adding to aromatic rings and abstracting H from C-H, O-H, or N-H bonds (Pignatello et al. 2006). Conversely, SO_4^- reacts with contaminants primarily through electron transfer mechanisms, such as H-atom abstraction and addition elimination, as described by Eqs. (32–33), respectively) (Padmaja et al. 1993). The specific reactions are as follows:



Therefore, a series of experiments on MNZ degradation was conducted at different pH values ranging from 3 ± 0.1 to 11 ± 0.1 to verify the influence of pH values on MNZ degradation. These experiments were conducted at an optimized temperature of 60°C and PS dosage of 20 mM; the pH value of the solution was adjusted to the target value by adding 0.1 M H_2SO_4 or NaOH without using other buffer solutions to avoid free radical quenching. The experimental data is shown in Fig. 4a. From the figure, MNZ degradation

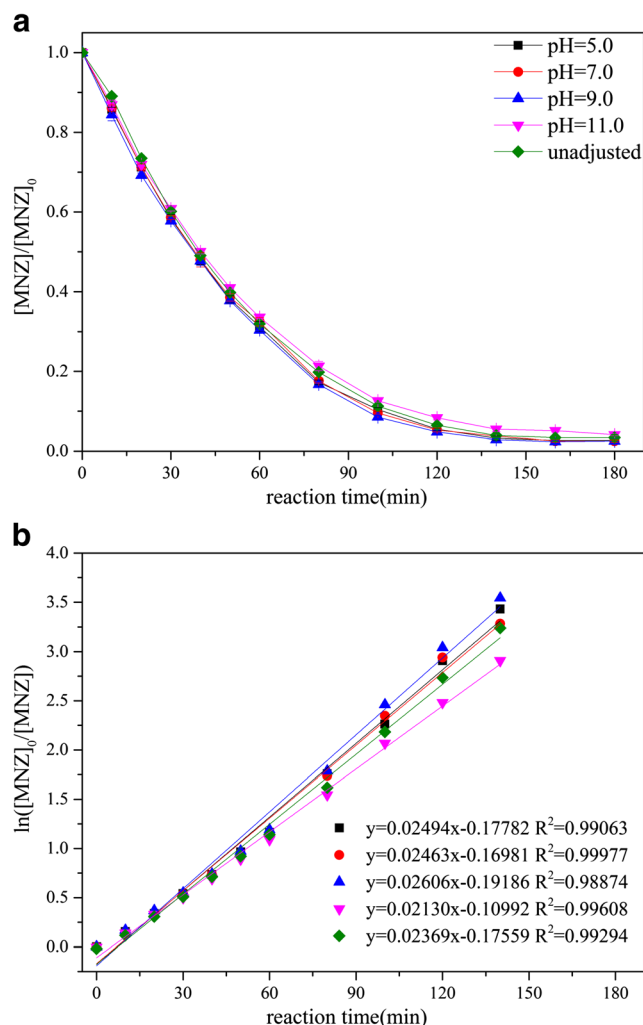


Fig. 4 a Effect of initial pH on MNZ degradation. b The pseudo-first-order kinetic reaction equations derived from a ($T = 60^\circ\text{C}$, $[PS]_0 = 20\text{ mM}$, $[MNZ]_0 = 100\text{ mg L}^{-1}$)

was observed to be following almost the same trend in all the pH conditions, considering that the effect of pH on MNZ degradation is subtle. As shown in Fig. 4b, the reaction rate constant was observed to be well-fitted with the pseudo-first-order kinetics model of $\text{pH } 9 > \text{pH } 7 \approx \text{pH } 5 > \text{unadjusted pH (approximately } 3) > \text{pH } 11$ ($R^2 > 98.8\%$). Similar enhanced oxidation of sulfamethazine and sulfonamides at weak basic condition was observed in ozonation (Fan et al. 2015). This result is plausibly attributed to the similar functional groups of MNZ (with nitro group) and sulfonamides (aniline moiety), thereby producing a withdrawing effect of electrons in the molecules (Fan et al. 2015). Moreover, MNZ by PAA/PVDF–NZVI hybrids and *p*-nitrophenol by TAP process has similar degradation trends at different pH values. As previously discussed, the TAP process oxidizes MNZ within a broad range of pH, which is of great significance for engineering applications.

Identification of dominating reactive radicals

At present, SO_4^- and HO^\cdot are considered as reactive oxidative species in the TAP process (Anipsitakis and Dionysiou 2004). To identify the contribution of these two radicals to MNZ degradation, classical quenching tests were conducted using MeOH and TBA as quenching agents in MNZ degradation. MeOH is a quenching agent containing R–H that can react with HO^\cdot at a second-order-rate constant of $(1.2–2.8) \times 10^9 \text{ M}^{-1} \text{ s}^{-1}$, which is approximately 50-fold higher than that of SO_4^- at $(1.6–1.7) \times 10^7 \text{ M}^{-1} \text{ s}^{-1}$. By contrast, TBA without R–H can effectively react with HO^\cdot at a high rate constant of $(3.8–7.6) \times 10^8 \text{ M}^{-1} \text{ s}^{-1}$, which is nearly 1000-fold higher than that of SO_4^- at $(4–9.1) \times 10^5 \text{ M}^{-1} \text{ s}^{-1}$ (Hussain et al. 2014). These quenching results are shown in Fig. 5a. The degradation efficiency of MNZ decreased from 96.6 to 15.3% with the addition of excess MeOH (20 M) during the 180-min reaction time; hence, most MNZ was oxidized by SO_4^- and HO^\cdot . Because the concentration of TBA cannot be continuously increased, thus, 8 M TBA was used to quench free radicals, and the inhibition efficiency of MNZ degradation was 40.9% with TBA. Therefore, 43.8% of degradation efficiency could be attributed to SO_4^- , whereas only 37.5% should be due to HO^\cdot . These results indicate that SO_4^- is the primary reactive radical dominating the MNZ degradation.

To further verify the reactive radicals in TAP process, the radical intermediates were identified through EPR experiments by adding the spin-trapping agent DMPO and comprehensively evaluating the absence of SO_4^- and HO^\cdot . As shown in Fig. 5b, the EPR spectrum was a composite spectrum of two different radical adducts, namely, DMPO– SO_4^- and DMPO– HO^\cdot adducts. The intensity of the characteristic peak was in accordance with those of DMPO– SO_4^- and DMPO– HO^\cdot adducts (Gao et al. 2016). Moreover, the intensity of DMPO– SO_4^- and DMPO– HO^\cdot adducts increased from approximately 250 to 2300 a.u. and from 50 to 300 a.u., respectively, with the increase of reactive time from 1 to 9 min. These results further confirmed that both SO_4^- and HO^\cdot were produced in TAP process.

MNZ mineralization analysis

An extended period of 10 h was conducted to analyze the mineralization of MNZ during the TAP process. Mineralization was tested for MNZ (100 mg L^{-1}) using a TOC analyzer. As shown in Fig. 6, an experimental TOC value of 45.86 mg L^{-1} was measured for non-treated MNZ. The measured value was consistent with the theoretical value of 42.12 mg L^{-1} , which was calculated by the molecular formula of MNZ ($(12.01 \times 6)/171.1$). Moreover, approximately

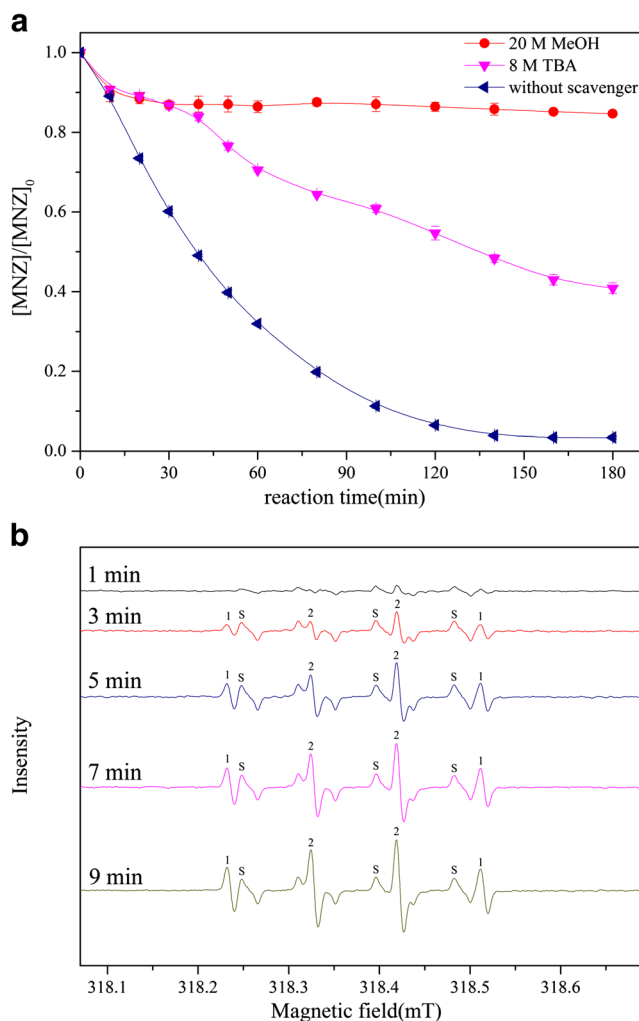


Fig. 5 a Effect of MeOH and TBA as radical scavengers on MNZ degradation. b EPR spectrum for TAP process in presence of DMPO (s represents the DMPO– SO_4^- and 1, 2, 2, 1 represent the four typical spectra of DMPO– HO^\cdot) (unadjusted pH, $T = 60 \text{ }^\circ\text{C}$, $[PS]_0 = 20 \text{ mM}$, $[MNZ]_0 = 100 \text{ mg L}^{-1}$)

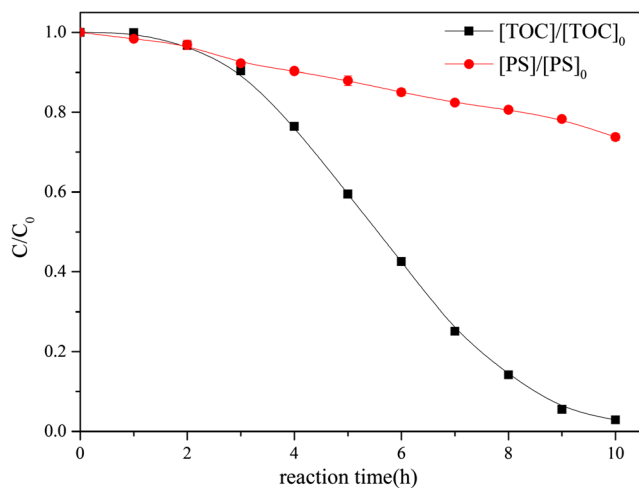


Fig. 6 Consumption of PS and mineralization of TOC on MNZ degradation (unadjusted pH, $T = 60 \text{ }^\circ\text{C}$, $[PS]_0 = 20 \text{ mM}$, $[MNZ]_0 = 100 \text{ mg L}^{-1}$)

97.2% of TOC removal (measured final TOC of 1.31 mg L⁻¹) was detected after 10 h at 60 °C. Compared with other methods for MNZ degradation, only 15% MNZ degradation was achieved by biological treatment and approximately 85% of TOC was removed by electrochemical reduction combined with biological treatment (Saidi et al. 2014). In contrast to the TOC removal of other pollutants by TAP process, approximately 11.5% of TOC removal was achieved after 8 h at 60 °C for triclosan degradation (Gao et al. 2016). These results indicate that the TAP process is a simple and effective method for realizing a complete MNZ mineralization.

Parallel to MNZ mineralization analysis, PS consumption was also detected in the TAP process. PS showed a relatively low consumption efficiency of 26.2% in the process, and PS concentration had a stable consumption rate. The results indicate that the pollutant was degraded continuously and stably. Thus, a greater concentration of MNZ could also be mineralized completely over time.

Conclusions

In this work, the effectiveness of TAP process in degrading MNZ in aqueous solutions was systematically investigated. MNZ degradation was well fitted with the pseudo-first-order kinetics by deriving and fitting experimental data simultaneously. Increasing the initial PS concentration or temperature considerably enhanced the degradation efficiency of MNZ; however, pH value did not significantly influence MNZ degradation. The degradation efficiency of MNZ reached 96.6% within 180 min for an initial MNZ concentration of 100 mg L⁻¹ under the optional condition of [PS]₀ = 20 mM, *T* = 60 °C, and unadjusted pH. Based on the results of the quenching experiment and EPR, SO₄⁻ and HO[•] were proven to be the main reactive radicals generated in the process. Moreover, SO₄⁻ played the dominant role in MNZ oxidation.

Acknowledgements This work was supported by the National Nature Science Foundation of China (Grant No. 41302184), Scientific Frontier and Interdisciplinary Research Project of Jilin University, Outstanding Youth Cultivation Plan of Jilin University, and Key Laboratory of Groundwater Resources and Environmental of Ministry of Education (Jilin University).

Compliance with ethical standards

Conflict of interest The authors declare that they have no conflict of interest.

Ethical statement This article does not contain any studies with human participants or animals performed by any of the authors.

References

- Ammar HB (2016) Sono-Fenton process for metronidazole degradation in aqueous solution: effect of acoustic cavitation and peroxydisulfate anion. *Ultrason Sonochem* 33:164–169
- Anipsitakis GP, Dionysiou DD (2004) Radical generation by the interaction of transition metals with common oxidants. *Environ Sci Technol* 38:3705–3712
- Antoniou MG, de la Cruz AA, Dionysiou DD (2010) Degradation of microcystin-LR using sulfate radicals generated through photolysis, thermolysis and e⁻ transfer mechanisms. *Appl Catal B Environ* 96: 290–298. <https://doi.org/10.1016/j.apcatb.2010.02.013>
- Azam A, Siraji F, Amran M, Islam J, Amjad F, Hossain M (2011) In vitro interaction of metronidazole and mebendazole with copper (II) and chromium (III) in aqueous media. *J Sci Res* 4:173–181
- Chen J et al (2012) Removal mechanism of antibiotic metronidazole from aquatic solutions by using nanoscale zero-valent iron particles. *Chem Eng J* 181–182:113–119. <https://doi.org/10.1016/j.cej.2011.11.037>
- Chen J, Qian Y, Liu H, Huang T (2016) Oxidative degradation of diclofenac by thermally activated persulfate: implication for ISCO. *Environ Sci Pollut Res* 23:3824–3833. <https://doi.org/10.1007/s11356-015-5630-0>
- Cheng W, Yang M, Xie Y, Liang B, Fang Z, Tsang EP (2013) Enhancement of mineralization of metronidazole by the electro-Fenton process with a Ce/SnO₂-Sb coated titanium anode. *Chem Eng J* 220:214–220. <https://doi.org/10.1016/j.cej.2013.01.055>
- Deng J, Shao Y, Gao N, Deng Y, Zhou S, Hu X (2013) Thermally activated persulfate (TAP) oxidation of antiepileptic drug carbamazepine in water. *Chem Eng J* 228:765–771
- Fan Y, Ji Y, Kong D, Lu J, Zhou Q (2015) Kinetic and mechanistic investigations of the degradation of sulfamethazine in heat-activated persulfate oxidation process. *J Hazard Mater* 300:39–47. <https://doi.org/10.1016/j.jhazmat.2015.06.058>
- Fang Z, Qiu X, Chen J, Qiu X (2010) Degradation of metronidazole by nanoscale zero-valent metal prepared from steel pickling waste liquor. *Appl Catal B Environ* 100:221–228. <https://doi.org/10.1016/j.apcatb.2010.07.035>
- Fang Z, Chen J, Qiu X, Qiu X, Cheng W, Zhu L (2011) Effective removal of antibiotic metronidazole from water by nanoscale zero-valent iron particles. *Desalination* 268:60–67. <https://doi.org/10.1016/j.desal.2010.09.051>
- Farzadkia M, Bazrafshan E, Esrafil A, Yang J-K, Shirzad-Siboni M (2015) Photocatalytic degradation of metronidazole with illuminated TiO₂ nanoparticles. *J Environ. Health Sci Eng* 13:35
- Furman OS, Teel AL, Watts RJ (2010) Mechanism of base activation of persulfate. *Environ Sci Technol* 44:6423–6428
- Gao H, Chen J, Zhang Y, Zhou X (2016) Sulfate radicals induced degradation of triclosan in thermally activated persulfate system. *Chem Eng J* 306:522–530. <https://doi.org/10.1016/j.cej.2016.07.080>
- Ghauch A, Tuqan AM, Kibbi N (2012) Ibuprofen removal by heated persulfate in aqueous solution: a kinetics study. *Chem Eng J* 197: 483–492
- Gómez MJ, Petrović M, Fernández-Alba AR, Barceló D (2006) Determination of pharmaceuticals of various therapeutic classes by solid-phase extraction and liquid chromatography–tandem mass spectrometry analysis in hospital effluent wastewaters. *J Chromatogr A* 1114:224–233
- Gómez MJ, Malato O, Ferrer I, Agüera A, Fernández-Alba AR (2007) Solid-phase extraction followed by liquid chromatography–time-of-flight–mass spectrometry to evaluate pharmaceuticals in effluents. A pilot monitoring study. *J Environ Monit* 9:718–729
- Gu X, Lu S, Li L, Qiu Z, Sui Q, Lin K, Luo Q (2011) Oxidation of 1,1,1-trichloroethane stimulated by thermally activated persulfate. *Ind Eng Chem Res* 50:11029–11036

- House DA (1962) Kinetics and mechanism of oxidations by peroxydisulfate. *Chem Rev* 62:185–203
- Hussain I, Zhang Y, Huang S (2014) Degradation of aniline with zero-valent iron as an activator of persulfate in aqueous solution. *RSC Adv* 4:3502–3511
- Ingerslev F, Torång L, Loke M-L, Halling-Sørensen B, Nyholm N (2001) Primary biodegradation of veterinary antibiotics in aerobic and anaerobic surface water simulation systems. *Chemosphere* 44:865–872. [https://doi.org/10.1016/s0045-6535\(00\)00479-3](https://doi.org/10.1016/s0045-6535(00)00479-3)
- Ji Y, Dong C, Kong D, Lu J, Zhou Q (2015) Heat-activated persulfate oxidation of atrazine: implications for remediation of groundwater contaminated by herbicides. *Chem Eng J* 263:45–54
- Kmmerer K (2001) Drugs in the environment: emission of drugs, diagnostic aids and disinfectants into wastewater by hospitals in relation to other sources—a review. *Chemosphere* 45:957–969
- Kolthoff I, Miller I (1951) The chemistry of persulfate. I. The kinetics and mechanism of the decomposition of the persulfate ion in aqueous medium. *J Am Chem Soc* 73:3055–3059
- Kümmerer K, Al-Ahmad A, Mersch-Sundermann V (2000) Biodegradability of some antibiotics, elimination of the genotoxicity and affection of wastewater bacteria in a simple test. *Chemosphere* 40:701–710
- Lee Y-C, Lo S-L, Kuo J, Lin Y-L (2012) Persulfate oxidation of perfluorooctanoic acid under the temperatures of 20–40 °C. *Chem Eng J* 198:27–32
- Liang C, Wang ZS, Bruell CJ (2007) Influence of pH on persulfate oxidation of TCE at ambient temperatures. *Chemosphere* 66:106–113. <https://doi.org/10.1016/j.chemosphere.2006.05.026>
- Liang C, Huang C-F, Mohanty N, Kurakalva RM (2008) A rapid spectrophotometric determination of persulfate anion in ISCO. *Chemosphere* 73:1540–1543
- Mahdi Ahmed M, Barbati S, Doumenq P, Chiron S (2012) Sulfate radical anion oxidation of diclofenac and sulfamethoxazole for water decontamination. *Chem Eng J* 197:440–447. <https://doi.org/10.1016/j.cej.2012.05.040>
- McCallum JE, Madison SA, Alkan S, Depinto RL, Rojas Wahl RU (2000) Analytical studies on the oxidative degradation of the reactive textile dye Uniblue A. *Environ Sci Technol* 34:5157–5164
- Mendez-Diaz JD, Prados-Joya G, Rivera-Utrilla J, Leyva-Ramos R, Sanchez-Polo M, Ferro-Garcia MA, Medellin-Castillo NA (2010) Kinetic study of the adsorption of nitroimidazole antibiotics on activated carbons in aqueous phase. *J Colloid Interface Sci* 345:481–490. <https://doi.org/10.1016/j.jcis.2010.01.089>
- Nie M, Yang Y, Zhang Z, Yan C, Wang X, Li H, Dong W (2014) Degradation of chloramphenicol by thermally activated persulfate in aqueous solution. *Chem Eng J* 246:373–382. <https://doi.org/10.1016/j.cej.2014.02.047>
- Olmez-Hanci T, Arslan-Alaton I, Genc B (2013) Bisphenol A treatment by the hot persulfate process: oxidation products and acute toxicity. *J Hazard Mater* 263:283–290
- Padmaja S, Alfassi Z, Neta P, Huie R (1993) Rate constants for reactions of radicals in acetonitrile. In *J Chem Kinet* 25:193–198
- Peyton GR (1993) The free-radical chemistry of persulfate-based total organic carbon analyzers. *Mar Chem* 41:91–103
- Pignatello JJ, Oliveros E, MacKay A (2006) Advanced oxidation processes for organic contaminant destruction based on the Fenton reaction and related chemistry. *Crit Rev Environ Sci Technol* 36:1–84
- Rivera-Utrilla J, Prados-Joya G, Sanchez-Polo M, Ferro-Garcia MA, Bautista-Toledo I (2009) Removal of nitroimidazole antibiotics from aqueous solution by adsorption/bioadsorption on activated carbon. *J Hazard Mater* 170:298–305. <https://doi.org/10.1016/j.jhazmat.2009.04.096>
- Rosal R et al (2010) Occurrence of emerging pollutants in urban wastewater and their removal through biological treatment followed by ozonation. *Water Res* 44:578–588. <https://doi.org/10.1016/j.watres.2009.07.004>
- Saidi I, Soutrel I, Floner D, Fourcade F, Bellakhal N, Amrane A, Geneste F (2014) Indirect electroreduction as pretreatment to enhance biodegradability of metronidazole. *J Hazard Mater* 278:172–179
- Sanchez-Polo M, Rivera-Utrilla J, Prados-Joya G, Ferro-Garcia MA, Bautista-Toledo I (2008) Removal of pharmaceutical compounds, nitroimidazoles, from waters by using the ozone/carbon system. *Water Res* 42:4163–4171. <https://doi.org/10.1016/j.watres.2008.05.034>
- Shemer H, Kunukcu YK, Linden KG (2006) Degradation of the pharmaceutical metronidazole via UV, Fenton and photo-Fenton processes. *Chemosphere* 63:269–276. <https://doi.org/10.1016/j.chemosphere.2005.07.029>
- Singh UC, Venkatarao K (1976) Decomposition of peroxydisulfate in aqueous alkaline solution. *J Inorg and Nuclear Chem* 38:541–543
- Szente V, Baska F, Zelkó R, Süvegh K (2011) Prediction of the drug release stability of different polymeric matrix tablets containing metronidazole. *J Pharm Biomed Anal* 54:730–734
- Tan C, Gao N, Deng Y, An N, Deng J (2012) Heat-activated persulfate oxidation of diuron in water. *Chem Eng J* 203:294–300
- Tsitonaki A, Smets BF, Bjerg PL (2008) Effects of heat-activated persulfate oxidation on soil microorganisms. *Water Res* 42(4):1013–1022
- Tsitonaki A, Petri B, Crimi M, Mosbæk H, Siegrist RL, Bjerg PL (2010) In situ chemical oxidation of contaminated soil and groundwater using persulfate: a review. *Crit Rev Environ Sci Technol* 40:55–91
- Wang X, Wang L, Li J, Qiu J, Cai C, Zhang H (2014) Degradation of Acid Orange 7 by persulfate activated with zero valent iron in the presence of ultrasonic irradiation. *Sep Purif Technol* 122:41–46
- Weng CH, Tsai KL (2016) Ultrasound and heat enhanced persulfate oxidation activated with Fe⁰ aggregate for the decolorization of C.I. Direct Red 23. *Ultrason Sonochem* 29:11–18. <https://doi.org/10.1016/j.ultsonch.2015.08.012>
- Xiao JC, Xie LF, Zhao L, Fang SL, Lun ZR (2008) The presence of *Mycoplasma hominis* in isolates of *Trichomonas vaginalis* impacts significantly on DNA fingerprinting results. *Parasitol Res* 102:613–619. <https://doi.org/10.1007/s00436-007-0796-0>
- Yan J, Lei M, Zhu L, Anjum MN, Zou J, Tang H (2011) Degradation of sulfamonomethoxine with Fe₃O₄ magnetic nanoparticles as heterogeneous activator of persulfate. *J Hazard Mater* 186:1398–1404. <https://doi.org/10.1016/j.jhazmat.2010.12.017>
- Yan J, Zhu L, Luo Z, Huang Y, Tang H, Chen M (2013) Oxidative decomposition of organic pollutants by using persulfate with ferrous hydroxide colloids as efficient heterogeneous activator. *Sep Purif Technol* 106:8–14. <https://doi.org/10.1016/j.seppur.2012.12.012>
- Yifei C, Shaojin C (2008) Reduction of methyl and chloro substituted nitrobenzenes in soils by zero-valent iron. *J Environ Sci Manag* 11: 017